Numerical Study of Thethermohydraulic and Energy-saving Performance of a Graphene Nanoplatelet-platinum Hybrid Nanofluid inside a Manifold Microchannel Heat Sink

■

Mohammad Reza Babaei[1], Ghanbar Ali Sheikhzadeh[2*], Ali Akbar Abbasian Arani[3]

■

[1] Faculty of Mechanical Engineering, University of Kashan, Kashan, Iran
mr.babaei60@gmail.com
[2] Faculty of Mechanical Engineering, University of Kashan, Kashan, Iran
sheikhz@kashanu.ac.ir
[3] Faculty of Mechanical Engineering, University of Kashan, Kashan, Iran
abbasian@kashanu.ac.ir

■

Abstract

Due to high heat flux in electronic equipment, the better cooling of these equipment using microchannel heat sink is of interest to many researchers today. However, paying attention to reducing energy consumption is also one of the essential issues that has attracted the attention of researchers and manufacturers.Thermohydraulic characteristics and energy saving of a water-based graphene nanoplatelet-platinum hybrid nanofluid inside a manifold microchannel heat sink for laminar flow have been investigated numerically for various nanofluid volume fractions (φ=0.02, 0.06, and 0.1%) and Reynolds number (Re=20 to 100). The Properties of hybrid nanofluid were considered temperature-dependent. According to studies conducted in this research, graphene nanoplatelet-platinum hybrid nanofluid in a manifold microchannel heat sink improves heat transfer performance. Cooling uniformity factor as a criterion for diagnosing of hotspot regions decreases with an increase in Reynolds number and nanofluid volume fraction. Nusselt number (Nu) increases with an increase in the Reynolds and nanofluid volume fraction. Nu_{max}=38.10 is obtained for Re=100 and φ=0.1% and Nu_{min}=24.17 is obtained for Re=20 and φ=0. Thermal resistance decreases with an increase in nanofluid volume fraction and Reynolds number. With an increase in Reynolds number andnanofluid volume fraction, pressure drop increases. Also, at low Reynolds numbers (Re=20), pressure drop differences in different volume fractions are insignifcant. For all nanofluid volume fraction values, the performane evaluation criterion (PEC) value is greater than 1, which indicates the improvement of manifold microchannel heat sink efficiency using nanofluids. Also, for all Reynolds values, the performance evaluation criterion with an increase in volume fraction increases. PEC_{max} for Re=20 and φ= 0.02% is achieved. There is no significant difference in the performance evaluation criterion for higher volume concentrations (0.06% and 0.1%) and higher Reynolds numbers (40 to 100).

Keywords: Manifold microchannel heat sink, thermohydraulic characteristics, graphene nanoplatelet – platinum (GNP-Pt), hybrid nanofluid, performance evaluation criterion (PEC).

---

1. Introduction

Today, the topic of cooling different equipment and devices and their thermal improvement is one of the important issues in research [1-4].

The manifold microchannel heat sink (MMHS) is an effective method for improving the thermal performance of electronic components in electronic equipment industry. Fig. 1 shows the MMHS schematic.
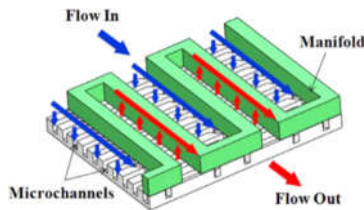

Fig. 1: Schematic of MMHS

According to Fig. 1, the length of the coolant path in the MMHS compared with the traditional microchannel heat sink is shortened, and cold fluid impinges on the microchannel bottom surface. As a result, the growth of the hydrodynamic and thermal boundary layers is decreased, the pressure drop is reduced, and the heat transfer is improved.

In electronics industry, various studies have focused on the use of MMHS to cool electronic chips.The following are a few of these studies.

Kermani [5] employed an experimental study to prove that the MMHS presented better heat exchange in cooling than the traditional microchannel heat sink (TMHS). His findings revealed that for MMHS, the microchannel having a hydraulic diameter (D_h=36μm) has 37% of the total pressure drop (Δp), while the microchannel with a hydraulic diameter (D_h=67μm) has 13% of the total pressure drop. The manifold is where the remaining entire pressure drop happens.

To study the performance of MMHS, the effects of geometric variables such as manifold input/output ratio, manifold height, and microchannel width were investigated by Sarangi et al. [6] using 3D numerical simulation. Porous-medium pattern and unit-cell pattern were two parts of their research. According to their findings, the manifold inlet/outlet ratio had to be equal to 3 at all times.

Drummond et al. [7] investigated a two-phase flow morphology in manifold microchannels with a high aspect ratio. Two-phase flow, played an essential role in heat exchange enhancement for manifold microchannels, according to their findings.

Yang et al. [8] compared a hybrid microchannel heat sink (HMHS) to a conventional manifold microchannel heat sink (CMMHS) in an experiment. The HMHS reduced thermal resistance and pressure drop, according to their findings.

Babaei et al. [9] numerically evaluated the impacts of changing geometric dimensions of MMHS on the heat transfer and flow field such as the height of the microchannel, inlet/outlet ratio length, and microchannel width at Reynolds number (Re) 20 to 100, to determine the ideal geometric dimension. The optimal geometry in terms of thermal improvement was selected based on the acquired results.Their results showed that the maximum performance evaluation criterion (PEC_{max}) for low Re is achieved at H_{ch}=300m, while PEC_{max} for high Re is obtained at H_{ch}=240m. PEC_{max} is 1.765 for Re=20 to 100, achieved at Re=100 and H_{ch}=240m.

In previous studies on MMHS, water has been used as the operating fluid. Today, to improve heat transfer, nanofluids are widely used because of their higher thermal conductivity in comparison with water [10-13]. Among nanoparticles such as metal oxide nanoparticles and carbon nanotubes, graphene (Gr) based materials, due to the very high thermal conductivity up to 5000 W/mK, have shown high potentials as nanoparticles; hence, today graphene is widely used in the cooling debate.

Ranjbarzadeh et al. [14] used a graphene oxide nanofluid to examine a circular copper tube's heat transport and friction coefficient .Compared to pure water, their results showed that the heat transfer coefficient increased by 40.3%, and the friction coefficient increased by 16% by employing graphene oxide nanofluid, resulting in a maximum thermal performance coefficient value of 1.148.

A procedure for producing functionalized graphene nanoplatelets nanofluid (fGNP) was devised by Sadri et al. [15]. This procedure was environmentally benign and simple. They discovered that compared to pure water, the heat transfer coefficient improved by 38.58%. Also, with nanofluid volume fraction ($φ$=0.1%), the Nusselt number (Nu) enhanced about 18.57%.

Esfahani et al. [16] used a modified Hummers method for preparing graphene oxide nanofluids to make graphene nano-sheets. In an experimental setting, they investigated the pressure drop and heat transfer comportment of graphene oxide nanofluid for flow inside a copper pipe at various flow rates and heat flux levels. According to their findings, the graphene oxide nanofluid with $φ$=0.01% had a greater heat exchange than the graphene oxide nanofluid with $φ$=0.1% and water,. They also discovered that the Nusselt number was unaffected by heat flux and flow rate. Many other studies have been done in this field [17-21].

Hybrid nanofluids are a new type of nanofluid that has recently attracted much attention. Obtaining a hybrid nanofluid will present favorable features of its ingredients, which will be helpful in various applications. [22-26]. Some researchers have used graphene-based nanofluids as a coolant for heat transfer increment. Some of these studies are as follows:

Yarmand et al. [27], by decorating silver on functionalized graphene nanoplatelets, made a graphene–silver hybrid nanofluid. They also experimentally studied the thermohydrodynamic characteristics and thermophysical properties of GNP-Ag/water hybrid nanofluid for flow inside stainless-steel tube. They discovered that the GNP-Ag hybrid nanofluid had more excellent thermal conductivity, resulting in better heat transmission. The intensification of the friction factor

was unimportant when compared to the benefits of heat transfer improvement. Improved experimental proposed relations founded on experimental data were presented by them to evaluate the Nusselt number and the coefficient of friction.Yarmand et al. [28] created a novel hybrid nanofluid by coating of GNP with platinum nanoparticles. It was discovered that by testing the thermophysical parametersof this novel nanofluid, at 40 °C and φ=0.1%, thermal conductivity improved by 17.7%.

Bahiraei and Hesmatian [29], for various liquid blocks and CPU cooling, analyzed the effect of graphene–silver hybrid nanofluid. Their result showed that compared with pure water, hybrid nanofluid in liquid blocks delivered better results.

Yarmand et al. [30], by using graphene-platinum nanoplatelet (GNP-Pt) hybrid nanofluid with $\varphi = 0.02\%$ to $\varphi = 0.1\%$, experimentally studied forced heat transfer inside a microchannel considering constant heat flux examined at Re=5000 to Re=1750,000. Their results showed that an essential enhancement of heat transfer in comparison with the base fluid was obtained using the above nanofluid so that a 30% enhancement in the highest Reynolds number and the highest volume fraction (Re=1750,000 and φ=0.1%) was obtained. Also, the highest coefficient of frictionwas equal to 10.98% and was related to the same Reynolds number and volume concentration. Using temperature-dependent properties, Bahiraei and Hesmatian [31] numerically examined the thermal and hydraulic features of Gr-Ag hybrid nanofluid inside two novel microchannel heat sinks. Their findings demonstrated that when nanofluid concentration and fluid velocity increased, surface temperature, maximum temperature, cooling uniformity, and pumping power decreased.

To enhance the heat exchange rate inside a minichannel, Bahiraei and Mazaheri [32] employed graphene–platinum hybrid nanofluid. They claimed that the superior features of this hybrid nanofluid improved heat transmission without significantly increasing pressure drop.

Bahiraei et al. [33] used a computer model to calculate the thermohydraulic performance of Gr-Ag hybrid nanofluid inside a microchannel heat sink. They discovered that the heat transfer coefficientimproved by growing the nanofluid volume fraction and Reynolds number; temperature uniformity also improved, and the temperature of the bottom surface lowered. However, nanofluid increased pumping power and the Reynolds number at greater nanofluid concentrations.

Khosravi et al. [34] numerically investigated the characteristics of the thermodynamics laws for the GNP-Pt hybrid nanofluid through a cylindrical microchannel liquid block. Their results showed that by growing the Reynolds number and volume fraction, the convection heat transfer coefficient enhanced. Moreover,the thermal entropy generation was reduced.

The energy, heat transfer, and flow characteristics efficiency of the GNP-Pt hybrid nanofluid in tubes were examined by Bahiraei et al. [35]. The effects of several parameters on the counter and co-swirling flows such as nanoparticle concentration and configuration type were investigated. Their findings revealed that as the concentration of nanoparticles enhanced, both pumping power and heat transfer increased in the studied configurations. Bahirai et al. [36] used a hybrid nanofluid including graphene-platinum (GNP-Pt) nano-sheets to determine the thermal characteristics and energy efficiency of a triple tube heat exchanger with a blade on its outer surface. Their findings revealed that increasing nanoparticle concentration, increasing blade height, and decreasing blade pitch increased the total heat transfer coefficient and heat transfer rate of the heat exchanger. They proposed a heat exchanger with a higher blade height and narrower pitch in the presence of a high volume fraction of nanoparticles to improve heat exchange.

Heat transfer and fluid flow of nanofluids in a square microchannel, trapezoidal and smooth circular were numerically modeled by Goodarzi et al. [37]. In their study, Graphene nanoplatelets silver/water were used as nanofluid. Solid nano-sheets made up a volume concentration of 0 to 0.1% of the total volume concentration. Their findings revealed that nanofluid could be used as a viable cooling fluid replacement for distilled water, which is commonly used in heat exchangers in electronic devices.

Balaji et al. [38] provided an experimental investigation on the convective heat transfer within a microchannel in the presence of nanofluids containing functional graphene (f-GnP) nano-sheets with a water-based nanofluid. They inspected the outcome of mass flow rate (5 gr/s to 30 gr /s) and nanoparticle concentration (0% and 0.2%) on Nusselt number, pressure drop, and heat transfer coefficient. Their results showed that using graphene nanoparticles decreased the heat wall temperature by 10°C and increased the convective heat transfer coefficient by 71% and the Nusselt number by 60%, while they increased the pressure drop compared with water fluid by 12%.
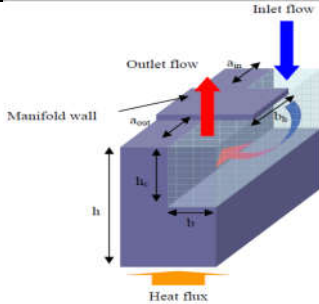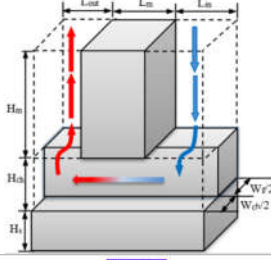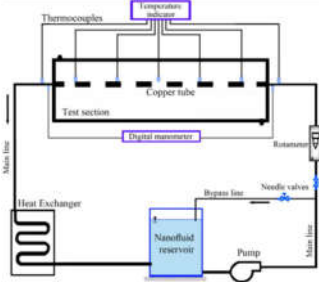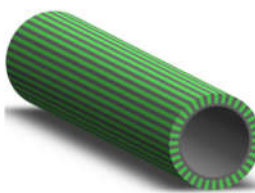
Khosravi et al. [39] numerically investigated heat transfer and fluid flow in a cylindrical microchannel in the presence of a GNP-Pt hybrid nanofluid. The results were evaluated for 4 Reynolds numbers with a volume fraction of 4%. Obtained results presented that the maximum PEC was 1.98 in volume concentration of $\varphi =$ 0.1%, Re=600, and the number of fins 36. Also, with growing each parameter of fins number, Reynolds number, and volume fraction, thermal resistance decreased. Table 1 shows some of the literature reviews with their main findings.

In all previous studies in the field of MMHS, the effects of temperature on the thermophysical properties of water and the body of microchannels and manifolds, generally made of silicon, were not investigated. Particularly, the changes in the thermal conductivity coefficient of silicon with respect to temperature, which were significant, were considered constant in all previous studies. Also, in the previous studies, the effects of different geometrical parameters on heat transfer and

pressure drop were investigated, but in none of them the effect of using hybrid nanofluid on the thermohydraulic performance of MMHS was investigated. In the present work, the above mentioned effects are considered. Also, in the previous studies in the field of MMHS, the performance evaluation criterion, as a valuable criterion for choosing the optimal conditions, was not mentioned, while most studies today use this criterion to select an appropriate economic model. In this work, the optimum volume fraction of nanoparticles are found using the definition of performance evaluation criterion.

The thermohydraulic properties of GNP-Pt in an MMHS are quantitatively examined in the current study at Re=20 to 100. The current examination begins with a presentation of the model under discussion and its boundary conditions. Afterwards, a set of governing equations, a numerical technique, a grid independency study, and validation are carried out. Finally, the research on fluid flow and heat transfer properties of laminar flow of a GNP-Pt in an MMHS is provided with findings and comments.

Table 1: Some of the literature reviews with their Main findings			
Reference	Research method	Configuration	Main findings
Kermani [5]	Experimental		The microchannel having ahydraulic diameter (Dh=36μm) has 37% of the total pressure drop (Δp) while the microchannel with a hydraulic diameter (Dh=67μm) has 13% of the total pressure drop.
Babaei et al. [9]	Numerical		PECmaxfor low Re is achieved at Hch=300m, while PECmax for high Re is obtained at Hch=240m. PECmax is 1.765 for Re=20 to 100, and it is achieved at Re=100 and Hch=240m.
Ranjbarzadeh et al. [14]	Experimental		Compared with pure water, the heat transfer coefficient increases by 40.3%, and the friction coefficient increases by 16% by employing graphene oxide nanofluid resulting in a maximum thermal performance coefficient value of 1.148.
Bahiraei et al. [32]	Numerical		The superior features of graphene–platinum hybrid nanofluid improved heat transmission without significantly increasing pressure drop.
Bahiraei et al. [31]	Numerical		When nanofluid concentration and fluid velocity increase, surface temperature, maximum temperature, cooling uniformity, and pumping power decrease.
Khosravi et al. [39]	Numerical		The maximum PEC is 1.98 in volume concentration of φ = 0.1%, Re = 600, and the number of fins is 36. Also, with growing each of the parameters of fins number, Reynolds number, and volume fraction, thermal resistance diminutions.

2. Geometrical Model Description

A schematic diagram of MMHS and the geometric dimension and computational domain of an MMHS unit cell are shown in Fig. 2(a andb). A unit cell of MMHS is selected due to the boundary condition of symmetry and reduction computation time. Mass flow inlet 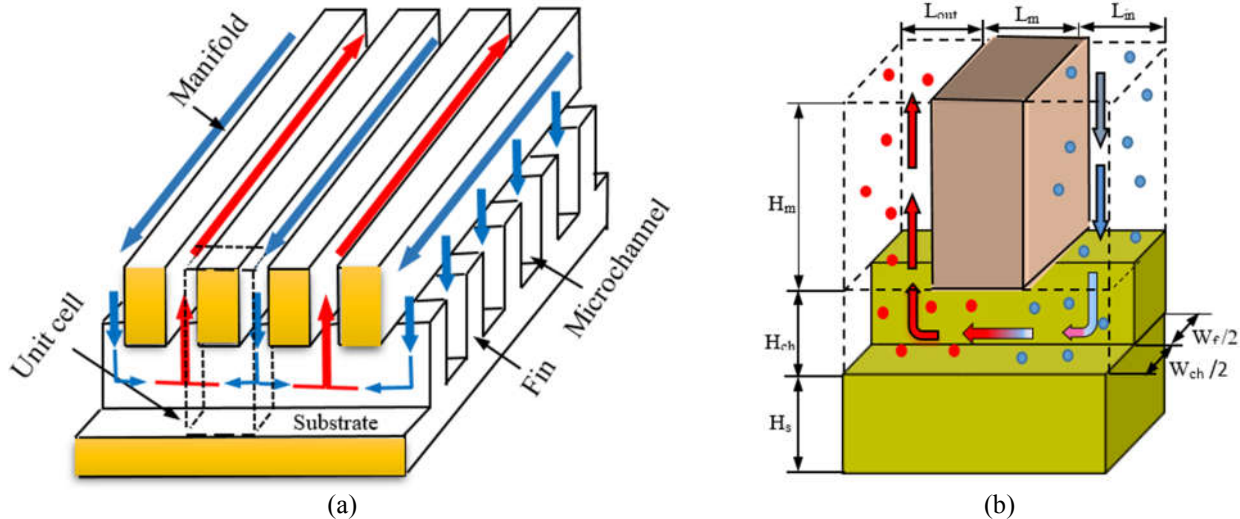and pressure outlet are chosen as boundary conditions at the manifold's inlet and outletrespectively. $q''=100W/cm^2$ is the microchannel bottom wall thermal boundary condition, and a boundary condition of non-slip velocity is considered for microchannel walls. The geometric dimensions of MMHS in this study are given in Table 2.

| (a) | (b) |

Fig. 2: (a) Schematic diagram of MMHS (b) Geometric dimension and computational domain

3. Properties of Silicon and Hybrid Nanofluid

Hybrid nanofluid in this study is used as a working fluid, made by dispersing platinum-coated graphene nanoplatelets (GNPs) in water. The thermal conductivity of this nanofluid is found to be 17.7% higher by Yarmand et al. [28], who synthesized it. The underlying liquid Graphene platelets have several beneficial features such as high thermal conductivity, high mechanical strength, and low density. Thermal conductivity, density, viscosity, and specific heat capacity are temperature-dependent thermophysical parameters. The thermophysical parameters of this nanofluid were experimentally measured by Yarmand et al. [28]. Bahiraei et al. [33] presented Mathematical equations of GNP–Pt nanofluidthermophysical properties according to the experimental data of Yarmand et al.. Table 3 shows these mathematical models. In the present modeling, the microchannels and manifold material are selected from silicon [36]. Considering the thermophysical properties of silicon and its effect on the outcome of the current investigation, the temperature-dependent coefficient of thermal conductivity of silicon is considered. Table 4 shows the thermophysical properties of silicon [40].

Table 2: Geometric dimensions of MMHS in this study (μm)							
H_{ch}	H_m	H_s	W_{ch}	W_f	L_{in}	L_{out}	L_m
400	360	1500	60	60	200	400	200

Table 3: Mathematical relation for GNP–Pt nanofluid properties [35]				
φ (%)	Density (kg/m^3)	Specific heat (J/kgK)	Thermal conductivity (W/mK)	Viscosity (kg/ms)
0	$1085.05 - 0.29689T$	$0.12T + 4065.8$	$0.0020338T - 0.0057$	$3.08212404044923 \times 10^{13} \times T^{-6.6681}$
0.02	$1086.6 - 0.3T$	$4261.2 - 0.7257143T$	$0.0026165T - 0.1689$	$1.37573089707629 \times 10^{12} \times T^{-6.107681}$
0.06	$1085.1 - 0.2943T$	$4248.1 - 0.7771T$	$0.0029T - 0.2336$	$7.04657066469 \times 10^{7} \times T^{-4.366}$
0.1	$1086.5 - 0.2979T$	$1.02T + 3492.5$	$0.0032T - 0.2646$	$3.5197010825669 \times 10^{8} \times T^{-4.63845}$

Table 4: Thermo-physical properties of silicon [40]		
Density(kg/m^3)	Specific heat (J/kgK)	Thermal conductivity (W/mK)
2330	706.83	$5385.987-55.38469T+0.2225836T^2-0.0004026317T^3+2.745317\times 10^{-7}T^4$

4. Governing Equations and Important Parameters

The hybrid nanofluid flow in this study is considered a laminar, steady state, considering variable (as a function of temperature) properties. Governing equations are as follows:

Continuity:

$$\nabla \cdot (\rho_{hnf} V) = 0 \tag{1}$$

Momentum equation:

$$\nabla \cdot (\rho_{hnf} VV) = -\nabla p + \nabla \cdot (\mu_{hnf} \nabla V) \tag{2}$$

Energy for the coolant:

$$\nabla \cdot (\rho_{hnf} V C p_{hnf} T) = \nabla \cdot (k_{hnf} \nabla T) \tag{3}$$

Energy for the solid region:

$$\nabla \cdot (k_{hnf} \nabla T) = 0 \tag{4}$$

T, p, and V refer to the temperature, pressure, and velocity vector. Subscripts s and hnf represent the solid and hybrid nanofluid respectively. Due to the consideration of the laminar flow regime, the Reynolds number is lower than 100.

The liquid in contact with the solid surface:

$$T_s = T_f \tag{5}$$

$$k_s \nabla T_s = k_f \nabla T_f \tag{6}$$

Parameters such as average Nusselt number (Nu), maximum temperature (T_{max}), thermal resistance (R_{th}), pressure drop (Δp), cooling uniformity (θ), average friction factor (f), and performance evaluation criterion (PEC) are analyzed to investigate the hydraulic thermal and characteristics.

The average friction coefficient is defined as:

$$f = 2\Delta p \frac{D_h}{L} \frac{1}{\rho u_{in}^2} \tag{7}$$

u_{in}, D_h, ρ, and L refer to the velocity, hydraulic diameter, density, and microchannel length respectively.

Nusselt number (average) is defined as:

$$Nu = \frac{q'' D_h}{k_{hnf} (\overline{T}_s - T_{mb})} \tag{8}$$

T_{mb} and $\overline{T}_s$ are themean bulktemperature and the average temperature of the microchannel wall respectively. The Performance Evaluation Criterion (PEC) is evaluated by:

$$PEC = (Nu_{hnf}/Nu_{bf})/(f_{hnf}/f_{bf})^{1/3} \tag{9}$$

In the above relation, subscript bf refers to the base fluid.

Cooling uniformity (θ) describes the consistency of temperature distribution over the substrate's bottom surface, which is defined as:

$$\theta = \frac{T_{max_{bs}} - T_{min_{bs}}}{q''} \tag{10}$$

Where $T_{max_{bs}}$ and $T_{min_{bs}}$ are the substrate bottom surface maximum and minimum temperatures.Cooling uniformity (θ) with a lower value indicates a more consistent temperature distribution on the substrate's bottom surface.

Thermal resistance (R_{th}) is a metric that is used to assess the heat sink's performance:

$$R_{th} = \frac{T_{max_{bs}} - T_{in}}{q''} \tag{11}$$

Where $T_{max_{bs}}$ and T_{in} are the substrate bottom surface maximum temperature and fluid temperature at the inlet of MMHS.

Flow in the straight segment of the microchannel is defined as:

$$Re = \frac{\dot{m}_{ch} D_h}{\mu_{hnf} A_{ch}} \tag{12}$$

Where

$$A_{ch} = w_{ch}/2 \times H_{ch} \tag{13}$$

$$D_h = \frac{2H_{ch} w_{ch}}{H_{ch} + w_{ch}} \tag{14}$$

5. Numerical Procedure

In this study, the finite volume-based flow solver ANSYS Fluent 18.2 is used to solve fluid flow and conjugate heat transfer in MMHS. A unit cell of MMHS is used to reduce the computational cost of each CFD simulation. Governing equations are solved via the second-order upwind method, and the pressure-velocity coupling via the SIMPLE algorithm. When the residual values of them are less than 10^{-6} for all variables, the numerical solutions are considered to be converged

5.1. Grid Independence Study

To ensure that the results are grid-independent, several meshes with various cell counts are employed. Fig.3 shows the results of the grid independency study in one situation and the variation of friction factor and temperature of three-point on the substrate bottom surface versus the number of elements. It can be seen from Fig.3 that acquired results do not show substantial differences when cell numbers are increased beyond 1420800. Therefore, a mesh with 1420800 cells is sufficient for performing simulation with grid-independent results.
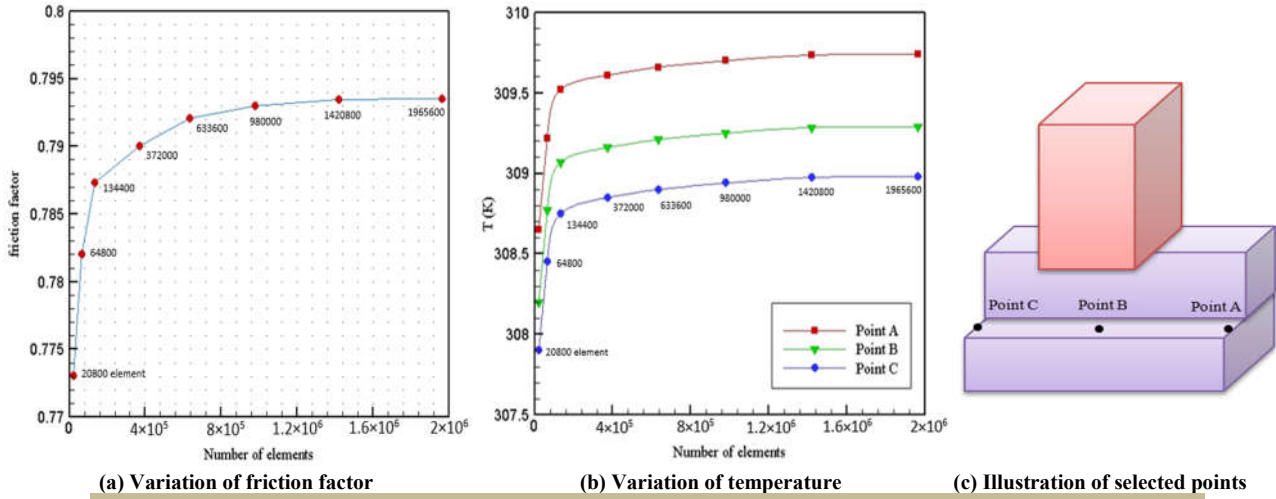
(a) Variation of friction factor   (b) Variation of temperature   (c) Illustration of selected points

Fig. 3: Grid independency study: Variation of friction factor and temperature versus the number of elements

5.2. Model Validation

The numerical findings are checked with existing experimental data to ensure the accuracy of numerical simulations. Fig. 4 shows the Kermani result (heat transfer coefficients) for D_h=67μm validation. This validation shows an acceptabel agreement between the present outcomes and Kermani experimental data [5].
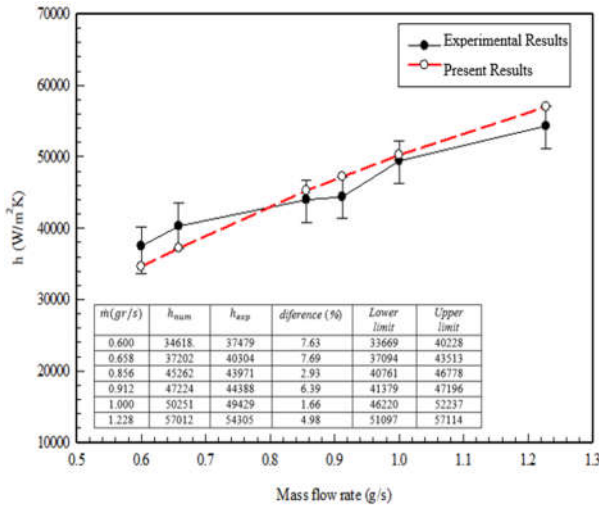

Fig. 4: Variations in heat transfer coefficients versus mass flow rate: A comparison of experimental results and numerical modeling for D_h=67μm[5]

6. Results and Discussion

This study has investigated the thermohydraulic properties of a GNP-Pt hybrid nanofluid in an MMHS at Re=20 to 100 using three-dimensional numerical simulations. Different volume concentrations (φ =0, 0.02, 0.06, and 0.1%) of a water-based GNP-Pt hybrid nanofluid at Re=20 to 100 have been simulated numerically. The $T_{max\,bs}$, Nu, θ, R_{th}, Δp, and f areused to determine the thermohydraulicof GNP–Pt hybrid nanofluid properties. The temperature contour of the MMHS is shown in Fig. 5 for various GNP-Pt hybrid nanofluid concentrations and Reynolds numbers.

According to Fig. 5, with an increase in φ, the temperature has decreased. From φ =0 to 0.1%, at Re=20, the maximum temprature from 312.79K to 311.58, at Re=60, from 309.01K to 308.59 K and at Re=100 from 308K to 307.66 K has been reduced. This is because in comparison with pure water, the thermal conductivity of the GNP-Pt hybrid nanofluid has been greater. Also, compared with base fluid, better cooling has been achieved for nanofluid with a larger volume concentration. By increasing the Reynolds number and, thus, the inlet velocity to the microchannel, more heat has been removed from the channel surface; as a result, the temperature has decreased. For example, at φ =0.1%, from R=20 to 100, the maximum temprature from 311.85K to 307.66K has been reduced. Fig. 6 shows the variation of $T_{max\,bs}$ with Re for φ =0, 0.02, 0.06, and 0.1%. From Fig. 6, it is observed that with the increase in Re and φ, $T_{max\,bs}$ has decreased. Also at higher Re, the reduction of the $T_{max\,bs}$ for different volume concentrations is not significant. From φ =0 to 0.1%, at Re=20, $T_{max\,bs}$ from 310.43K to 309.5K, at Re=60, from 306.66K to 306.25K and at Re=100 from 305.66K to 305.33K has been reduced. Atφ =0.1%, from R=20 to 100,$T_{max\,bs}$ from 309.5K to 305.33K has been reduced. Hybrid nanofluid with φ =0.1% and at Re=100 shows the lowest value for $T_{max\,bs}$, i.e., $T_{max\,bs}$ = 305.33 K. This is while the highest value for the substrate is 310.43K in Re=20 and for base fluid.

Checking the uniformity of the substrate bottom surface is essential to obtain hotspot regions. Therefore, a parameter called "cooling uniformity (θ)", expressed according to Equation 10, has been evaluated in various Re and φ. Fig. 7 shows the variation of θ with Re for φ =0, 0.02, 0.06, and 0.1%. This is a crucial point to know that better uniform temperature distribution has been obtained for θ close to zero.
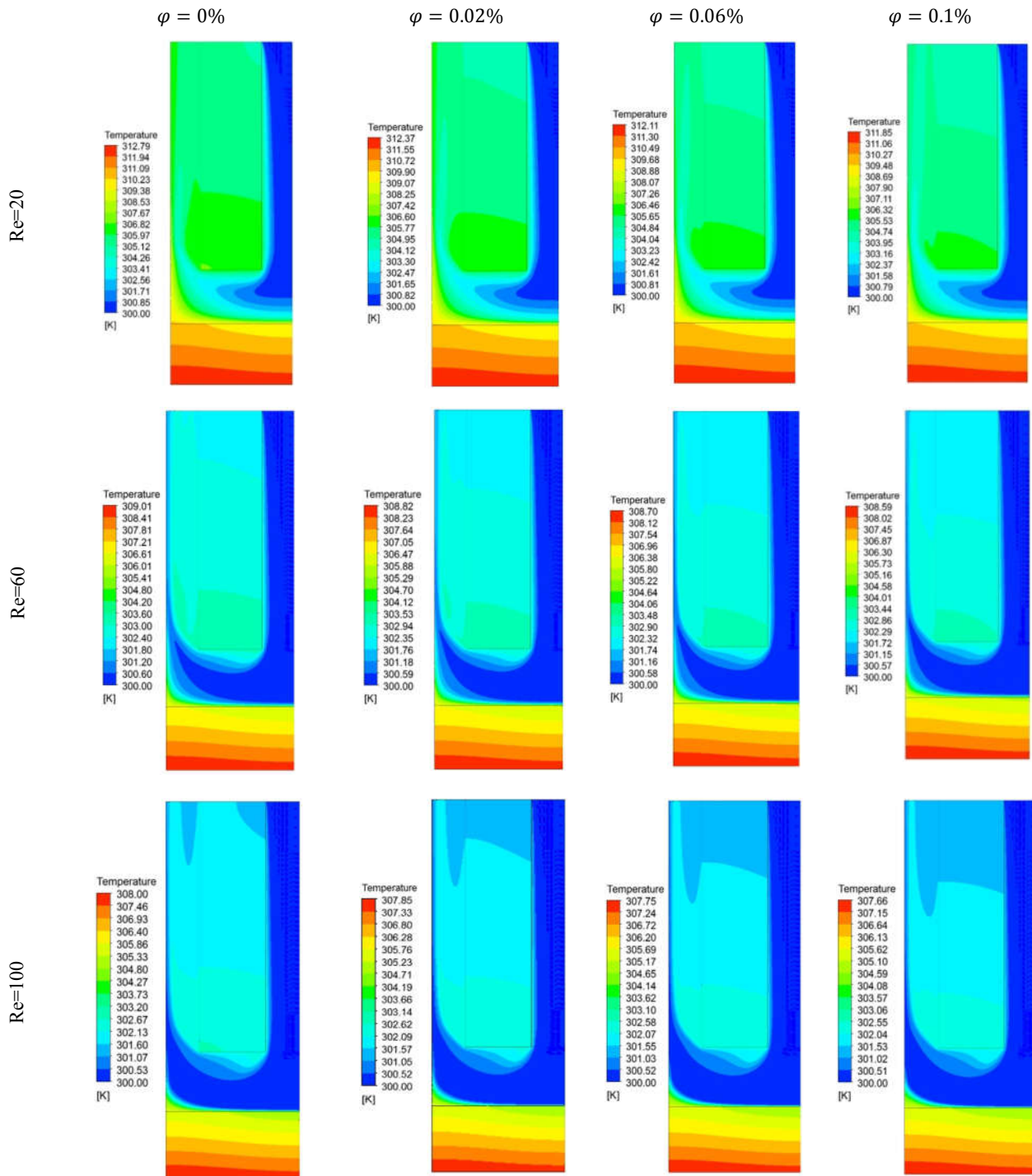
Fig. 5: Temperature contours for the middle section of MMHS varying volume concentrations (φ) at various Re

As seen from Fig.7, at lower Reynolds numbers (Re=20 and Re=40), with an increase in the volume fraction of nanoparticles, the cooling uniformity coefficient has decreased This decrease for Re=20 compared to Re=40 has been more prominent. At higher Reynolds numbers (Re=60, Re=80 and Re=100), with an increase in the volume fraction of nanoparticles, there has been no significant change in the value of the cooling uniformity coefficient, and an increase in the volume fraction of nanoparticles has not significantly contributed to the uniformity of cooling. However, increasing the Reynolds number from 20 to 40 has caused a decrease in the cooling uniformity coefficient and a more uniform temperature distribution on the target surface. From Reynolds number 40 onwards, the cooling uniformity coefficient has an almost constant value, and increasing the Reynolds number has not had a significant effect on the more uniformtemperature distribution. Fig. 8 shows the substrate bottom surface temperature contours for Re=20, Re=60 and Re=100 for φ=0 to φ=0.1%. substrate bottom surfaceis shown in fig. 2(a).
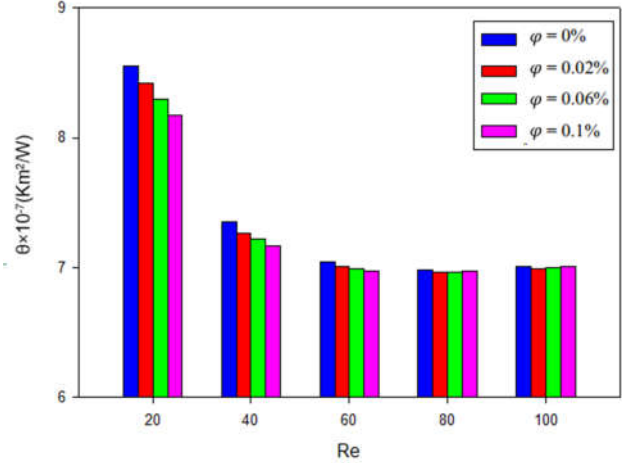
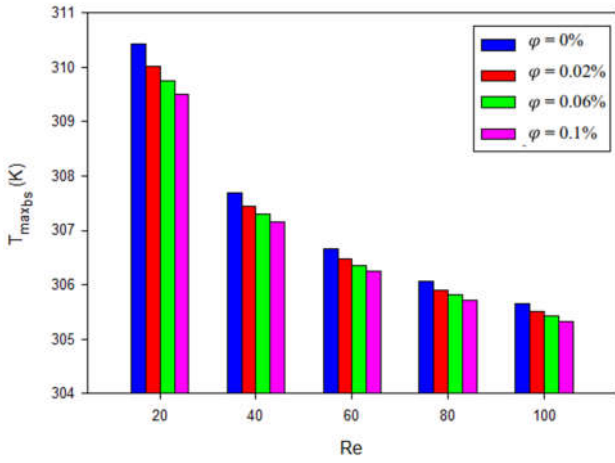**Fig. 6: Variation of $T_{max_{bs}}$ versus Re for various φ**

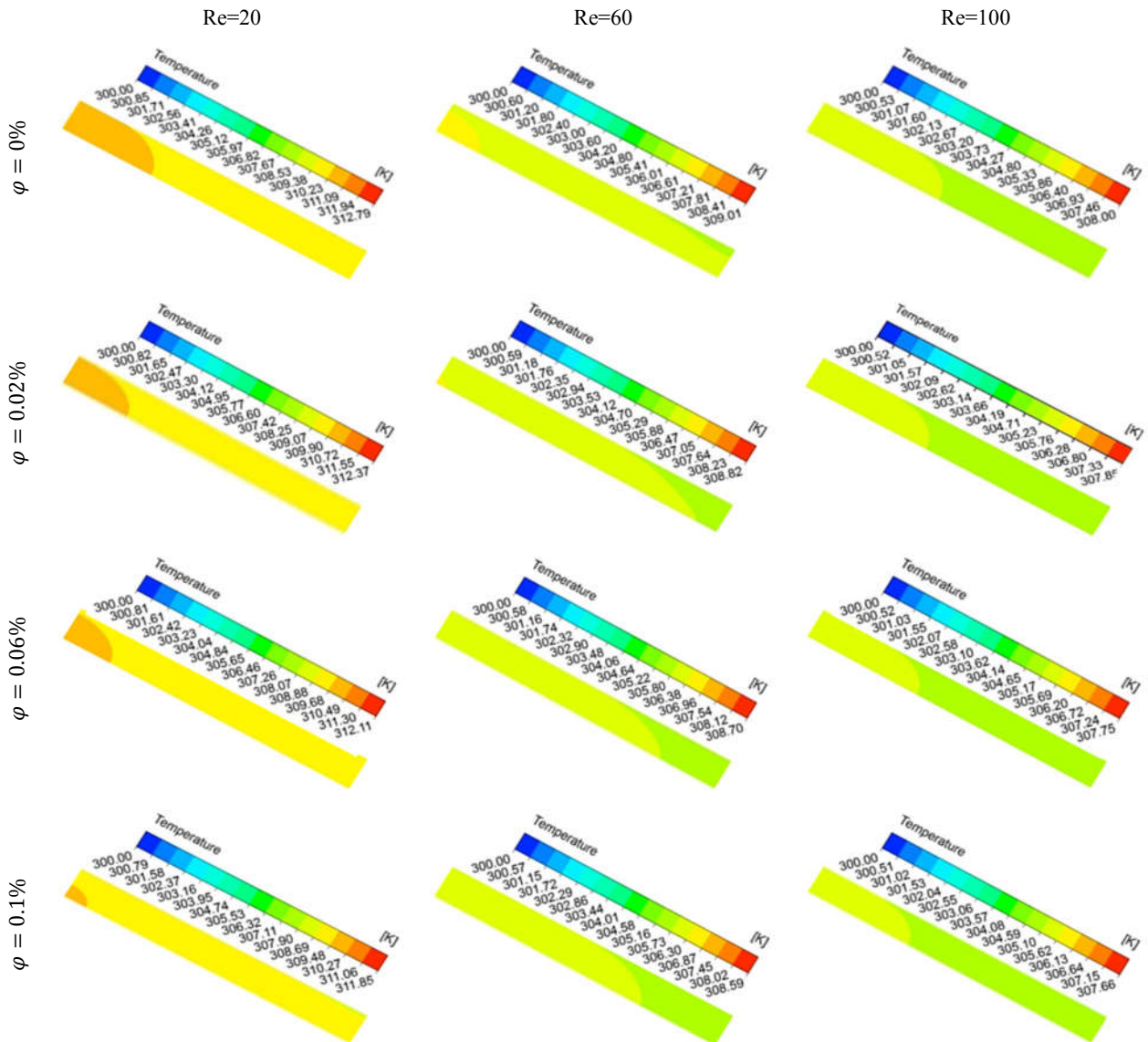**Fig. 7: Variation of θ versus Re for various φ**

Fig. 8: Temperature contour of the $T_{max_{bs}}$ for various φ and Re for substrate bottom surface

According to the fig.8, it can be seen that with an increase in the Reynolds number, the temperature values in the substrate bottom surface has decreased. Also, the temperature was lower at the beginning of the substrate bottom surface where the cooling fluid jet hits; with an increase in the length of the plane, the temperature value has increased. Also, with an increase in the volume fraction of nanoparticles, the temperature values in the substrate bottom surface has decreased. The changes in temperature with an increase in volume fraction of nanoparticles hace been lower compared to the changes in temperature due to an increase in Reynolds number. With a simultaneous increase of Reynolds number and volume fraction of nanoparticles, the hot spot area of the plate has decreased.

Fig. 9 shows the variation of the Nu with Re for φ =0, 0.02, 0.06, and 0.1% of GNP-Pt hybrid nanofluid. From Fig. 9, it is observed that the Nu has enhanced with an increase in the Re; in fact, when the inlet velocity enhances, the fluid's convective heat transport increases; it increases the convective heat transfer coefficient and, thus, increases the average Nu. Also, from Fig. 9, it can be seen that the Nu has increased with φ. This is related to the fact that the φ enhances, nanofluid thermal conductivity and heat transfer coefficient increase. Also, compared with that, in thermal conductivity, the percentage increment in the heat transfer coefficient has been more. Nu_{max}=38.10 is obtained for Re=100 and $\varphi = 0.1\%$ and Nu_{min}=24.17 is obtained for Re=20 and $\varphi = 0\%$. Fig. 10 shows the variation of R_{th} with Re for φ =0, 0.02, 0.06, and 0.1% of GNP–Pt hybrid nanofluid. From Fig. 10, it is observed that R_{th} has decreased with an increase in φ. According to Fig. 6 and the previous contents, it is found that with increasing the φ, $T_{max_{bs}}$ has decreased, and, thus, R_{th} has decreased according to Equation 11,. Furthermore, with an increase in Re, R_{th} has

decreased. The reason for this is that as the inlet velocity enhances, the fluid's convective heat transport increases, increasing the coefficient of convective heat transfer. As a result, the convective thermal resistance decreases, which results in decreased total thermal resistance.

Fig. 11 shows the variation of Δp with Re for φ =0, 0.02, 0.06, and 0.1% of Gr-Pt hybrid nanofluid. From Fig. 11, it is observed that with increasingφ, Δp has increased. This is because with increasing in φ, the viscosity of nanofluid increases, and, thus, Δp increases. Furthermore, Δp increases with enhancing Re. This is related to the fact that an enhancement in velocity gradient causes greater wall shear stress and increases Δp. Figure 12 shows the friction factor with Re for φ =0, 0.02, 0.06, and 0.1% of Gr–Pt hybrid nanofluid. From this figure, it is observed that as the Re has increased, the value of the friction factor had decreased. This is because the friction factor is related to pressure drop and inversely the square of fluid inlet velocity, as defined in Equation 7. It is also observed that in low Re, the friction factor has increased from $\varphi = 0$ to 0.02% and, then, decreases, but in high Re, the value of the friction factor has been close to each other for different φ.

Fig. 13 shows the variation of the performance Evaluation Criterion parameter (PEC) with Re for φ =0, 0.02, 0.06, and 0.1% of Gr–Pt hybrid nanofluid. From Fig. 13, it is observed that for all φ values, the PEC value is greater than 1, which indicates an improvement of MMHS efficiency using nanofluids. Of course, PEC values are small values. Also, for all Re, PEC with increasing φ increases. For $\varphi = 0.02\%$, the amount of PEC for different Re is close to each other, but for φ =0.06%, for Re=20 to 40, PEC is reduced, and after Re=40, the values are close to each other. The values, then, converge. The maximum value of PEC is 1.09 for φ =0.02 and Re= 20.
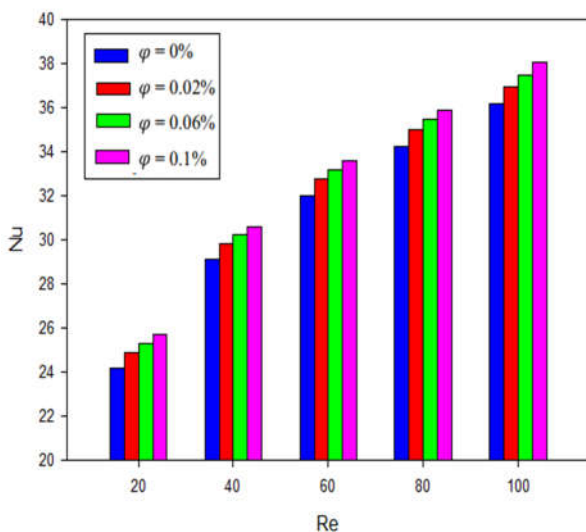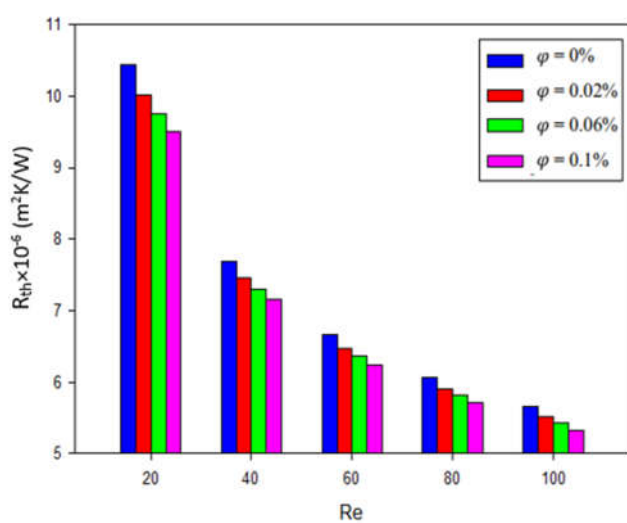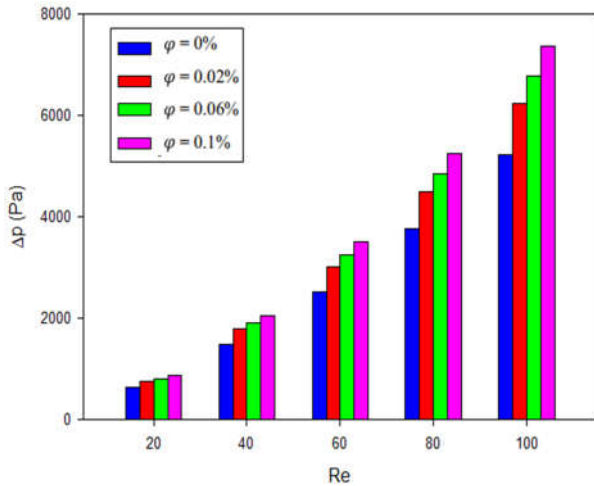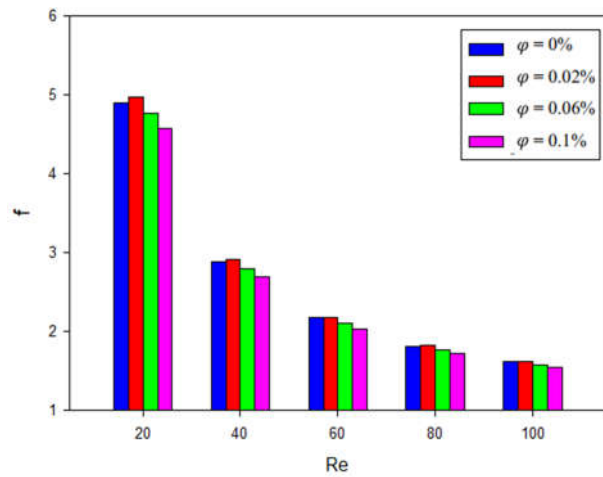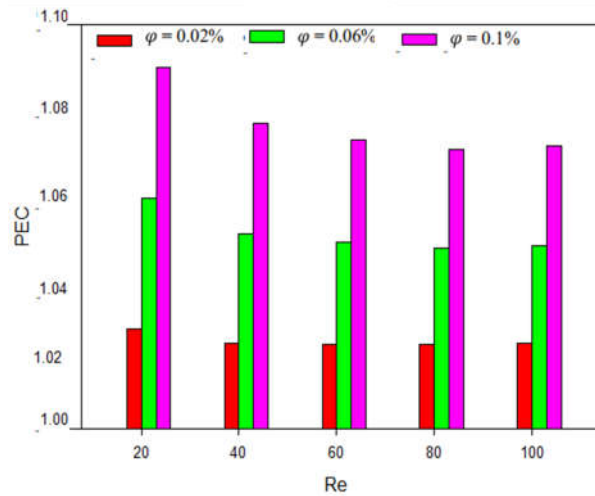

Fig. 9: Variation of Nu versus Re for various φ

Fig. 10: Variation of R_{th}versus Re for various φ

Fig. 11: Variation of Δp versus Re for various φ

Figure 12: Variation of f versus Re for various φ

Fig. 13: Variation of PEC versus Re for various φ

8. Conclusion

In this study, 3D numerical modeling was conducted in an MMHS to examine the thermohydraulic characteristics of GNP–Pt hybrid nanofluid with temperature-dependent thermophysical properties. φ =0 to 0.1% and Re=20 to 100 on the thermohydraulic performance in MMHS were examined. This study's main findings are as follows:

- With an increase both in Re and φ, $T_{max_{hs}}$ decreases. Also, at higher Re, the reduction of the $T_{max_{hs}}$ for different volume concentrations is not significant. The hybrid nanofluid with φ =0.1% and at Re=100 shows the lowest value for $T_{max_{hs}}$; that is, $T_{max_{hs}}$ = 305.32 K. This is while the highest value is $T_{max_{hs}}$ = 310.43 K for the base fluid at Re=20.

- Cooling uniformity, as a criterion for diagnosis of hotspot regions, decreases with both Re and φ. Also, as the Re increases, the change in cooling uniformity with φ becomes less noticeable.

- Nu increases with increasing the Re and φ. Nu_{max}=38.10 is obtained for Re=100 and φ=0.1% and Nu_{min}=24.17 is obtained for Re=20 and φ=0%.

- R_{th} decreases with an increase both in φ and Re. The difference of R_{th} in Re=20 is greater than other Re; and at the higher Re, the difference in R_{th} together becomes less.

- With an increase in Re and φ, Δp increases. Also, at low Re (Re=20), Δp differences in different φ are close to each other.

- As the Re increases, the value of the friction factor decreases. In low Re, the friction factor increases from φ=0 to 0.02%, and, then, decreases; however, in high Re, the value of the friction factor is close to each other for different φ.

- For all φ values, the PEC value is greater than 1, which indicates an improvement on MMHS efficiency using nanofluids. Also, for all Re values, PEC increases with increasing φ increases. PEC_{max} for Re=20 and φ= 0.02% is achieved. There is no significant difference in PEC for higher φ (0.06% and 0.1%) and higher Re (40 to 100).

NOMENCLATURE

A	Cross-section area (m^2)	**Subscripts**	
c_p	Specific heat capacity (J/kg K)	ch	Microchannel
f	Average friction coefficient	f	Fin
H	Height (μm)	hnf	Hybrid nanofluid
k	Thermal conductivity (W/m.K)	in	Inlet
L	Length (μm)	mb	Mean bulk
$\dot{m}$	Mass flow rate (kg/s)	max	Maximum
Nu	Average Nusselt number	min	Minimum
p	Pressure (Pa)	m	Manifold
q''	Heat flux (W/m^2)	out	Outlet
Re	Reynolds number	s	Substrate
R_{th}	Thermal resistance (Km^2/W)	**Abbreviations**	
T	Temperature(K)	CMMHS	Conventional manifold microchannel heat sink
V	Velocity vector(m/s)	FFMHS	Force-fed microchannel heat sink
W	Width (μm)	GNP	Graphene nanoplatelets
Greek symbols		JIHS	Jet impingement heat Sink
θ	Cooling uniformity (Km^2/W)	MMHS	Manifold microchannel heat sink
μ	Dynamic viscosity (Pa.s)	MMHE	Manifold microchannel heat exchanger
ρ	Density (Kg/m^3)	PEC	Performance evaluation criterion
φ	Nanofluid volume concentration	TMHS	Traditional microchannel heat sink

References

[1] Sheikhzadeh, G., Arbaban, M., "*Natural Convection of Cu-water Nanofluid in Concentric Annuli with Six Radial Fins Attached to Inner Cylinder*", Journal of Energy Engineering & Management, Vol. 2, No.2, pp. 52-61, 2012, (In persian).

[2] Mortazavi, h., ahmadi, A., bayareh, M., "*Feasibility of Usage Recovery Heat Exchanger in Vapor Compression Refrigeration Cycle by Using Thermodynamic, Heat Transfer and Economic Analyses*", Journal of Energy Engineering & Management, Vol. 8. No. 3, pp. 28-39, 2018, (In persian), doi:10.22052/8.3.28.

[3] Izadi, S., Mostajeran Goortani, B., alemrajabi, A. A. A., "*Study of Heller Cooling Towers and Increasing their Efficiency, Case Study: Shahid Mohammad Montazeri Power Plant*", Journal of Energy Engineering & Management, Vol. 8. No. 4, pp. 50-61, 2019, (In persian), doi:10.22052/8.4.50.

[4] Shahsavar, A., "*Experimental Investigation of Thermal and Electrical Performances of a Nanofluid-cooled Photovoltaic/Thermal System Equipped with a Sheet-and-grooved Serpentine Tube Collector*", Journal of Energy Engineering & Management, Vol. 12. No. 1, pp. 120-129, 2022, (In persian), doi: 10.22052/12.1.120.

[5] Kermani, E., "Manifold micro-channel cooling of photovoltaic cells for high-efficiency solar energy conversion", M.S. Thesis, University of Maryland, 2008.

[6] Sarangi, S., Bodla, K.K., Garimella, S.V., Murthy, J.Y., "*Manifold microchannel heat sink design using optimization under uncertainty*", International Journal of Heat and Mass Transfer, Vol. 69, pp. 92–105, 2014, doi:10.1016/j.ijheatmasstransfer.2013.09.067.

[7] Drummond, K.P., Back, D., Sinanis, M.D., Janes, D.B., Peroulis, D., Weibel, J.A., Garimella, S.V., "*A Hierarchical Manifold Microchannel Heat Sink Array for High-Heat-Flux Two-Phase Cooling of Electronics*", International Journal of Heat and Mass Transfer, Vol. 117, pp. 319–330, 2018, doi: 10.1016/j.ijheatmasstransfer.2017.10.015.

[8] Yang, M., Cao, B.Y., "*Numerical study on flow and heat transfer of a hybrid microchannel cooling scheme using manifold arrangement and secondary channels*", Applied Thermal Engineering, Vol. 159, 2019, doi: 10.1016/j.applthermaleng. 2019.113896.

[9] Babaei, M., Sheikhzadeh, G., Abbasian Arani, A., "*Numerical Investigation of Geometric Parameters Effects on Heat Transfer Enhancement in a Manifold Microchannel Heat Sink*". International Journal of Engineering, Vol.35, No. 5, pp. 943-953, 2022, doi: 10.5829/ije.2022.35.05b.10.

[10] Akbarzade, S., Sedighi, K., Farhadi, M., Ebrahimi, M., "*Experimental Investigation of Forced Convection Heat Transfer in a Car Radiator Filled with SiO2-Water Nanofluid*", International Journal of Engineering, Vol. 27, No.2,pp. 333-340, 2014, doi:10.5829/idosi.ije.2014.27.02b.17.

[11] Alagappan, N., Karunakaran, N., "*Performance Investigation of 405 Stainless Steel Thermosyphon using Cerium (IV) Oxide Nano Fluid*", International Journal of Engineering, Vol. 30, No.4,pp. 575-581,2017, doi: 10.5829/idosi.ije.2017.30.04a.16.

[12] Amirabedia, M., Jafarmadar, S., Khalilarya, S., Kheyrollahi, J., "*Experimental Comparison the Effect of Mn$_2$O$_3$ and Co$_3$O$_4$ Nano Additives on the Performance and Emission of SI Gasoline Fueled with Mixture of Ethanol and Gasoline*", International Journal of Engineering, Vol. 32, No.5,pp. 769-776, 2019, doi:10.5829/ije.2019.32.05b.19.

[13] Rahimian, A., Kazeminejad, H., Khalafi, H., Mirvakili, S., Akhavan, A., "*An Experimental Study of the Steel Cylinder Quenching in Water-based Nanofluids*", International Journal of Engineering, Vol. 33, No.1, pp. 28-33,2020, doi:10.5829/ije.2020.33.01a.04.

[14] Ranjbarzadeh, R., Karimipour, A., Afrand, M., Isfahani, AHM., Shirneshan, A., "*Empirical analysis of heat transfer and friction factor of water/graphene oxide nanofluid flow in turbulent regime through an isothermal pipe*", Applied

Thermal Engineering, Vol. 126, pp. 538-547, 2017, doi: 10.1016/j.applthermaleng.2017.07.189.

[15]Sadri, R., Hosseini, M., Kazi, S.N., Bagheri, S., Ahmed, S.M., Ahmadi, G., Zubir, N., Sayuti, M., Dahari, M., "*Study of environmentally friendly and facile functionalization of graphene nanoplatelet and its application in convective heat transfer*", Energy Conversion and Management, Vol. 150, pp. 26-36, 2017, doi: 10.1016/j.enconman.2017.07.036.

[16] Esfahani, M.R., Nunna, M.R., Languri, E.M., Nawaz, K., Cunningham, G., "*Experimental study on heat transfer and pressure drop of in-house synthesized graphene oxide nanofluids*", Heat Transfer Engineering, pp. 1722-1735, 2018, doi: 10.1080/01457632.2018.1497001.

[17] Ranjbarzadeh, R., Meghdadi Isfahani, A.H., Afrand, M., Karimipour, A., Hojaji, M., "*An experimental study on heat transfer and pressure drop of water/graphene oxide nanofluid in a copper tube under air cross-flow: Applicable as a heat exchanger*", Applied Thermal Engineering, Vol. 125, pp. 69-79, 2017, doi: 10.1016/j.applthermaleng.2017.06.110.

[18] Paramashivaiah, B., Rajashekar, C., "*Studies on Effect of Injection Timing of Graphene Nanoparticles Blended Simarouba Biodiesel Blend on CI Engine*", International Journal of Engineering, Vol. 30, No.8,pp. 1205-1214, 2017, doi: 10.5829/ije.2017.30.08b.13.

[19] Bahaya, B., Johnson, D. W., Yavuzturk, C. C., "*On the Effect of Graphene Nanoplatelets on Water–Graphene Nanofluid Thermal Conductivity, Viscosity, and Heat Transfer Under Laminar External Flow Conditions*", Journal of Heat Transfer, Vol. 140, 2018, doi: 10.1115/1.4038835.

[20] Narendran, G., Gnanasekaran, N., Perumal, D. A., "*Experimental Investigation on Heat Spreader Integrated Microchannel Using Graphene Oxide Nanofluid*", Heat Transfer Engineering, Vol. 41, NO.14, pp. 1252-1274,2020, doi: 10.1080/01457632.2019.1637136.

[21] Ong, Y.S., Shaari, K.Z.K., Laziz, A.M., Lu, I.L., Mohamad, M.F.R.S., Sufian, S., "*Thermal Performance of Graphene Oxide Nanofluid in Microchannel Heat Exchanger*", Journal of Enhanced Heat Transfer, Vol. 27, pp. 439–461, 2020, doi: 10.1615/JEnhHeatTransf.2020033046.

[22] Younis, A., Elsarrag, E., Alhorr, Y., Onsa, M., "*The influence of Al_2O_3-ZnO-H_2O nanofluid on the thermodynamic performance of photovoltaic-thermal hybrid solar collector system*", Innovative Energy & Research, Vol. 7, No.1, 2018, doi: 10.4172/2576-1463.1000187.

[23] Sheikhzadeh, G.A., Barzoki, F., Abbasian, A.A.A., Pourfattah, F., "*Wings shape affects the behavior of hybrid nanofluid inside a channel having a vortex generator*", Heat and Mass Transfer, Vol. 55, pp. 1969–1983, 2019, doi: 10.1007/s00231-018-2489-x.

[24] Abbasian, A.A.A., Monfaredi, F., Aghaei, A., Afrand, M., Chamkha, A.J., Emami, H., "*Thermal radiation effect on the flow field and heat transfer of Co_3O_4-diamond/EG hybrid nanofluid using experimental data: A numerical study*". The European Physical Journal Plus, Vol. 134, 2019, doi:10.1140/epjp/i2019-12431-7.

[25]Kumar, V., Sarkar J., "*Particle ratio optimization of Al_2O_3-MWCNT hybrid nanofluid in minichannel heat sink for best hydrothermal performance*", Applied Thermal Engineering, Vol. 165, pp. 1359-4311, 2020, doi: 10.1016/j.applthermaleng.2019.114546.

[26] Abbasian, A.A.A., Aberoumand, H., "*Stagnation-point flow of Ag-CuO/water hybrid nanofluids over a permeable stretching/shrinking sheet with temporal stability analysis*", Powder Technology, Vol. 380, 152-163. 2021, doi: 10.1016/j.powtec.2020.11.043.

[27]Yarmand, H., Gharehkhani, S., Ahmadi, G., Shirazi, S.F.S., Baradaran, S., Montazer, E., Zubir, M.N.M., Alehashem, M.S, Kazi, S.N., Dahari, M., "*Graphene nanoplatelets–silver hybrid nanofluids for enhanced heat transfer*", Energy Conversion and Management, Vol. 100, pp. 419-428, 2015, doi: 10.1016/j.enconman.2015.05.023.

[28]Yarmand, H., Gharehkhani, S., Shirazi, S.F.S., Goodarzi, M., Amiri, A., Sarsam, W.S., Alehashem, M.S., Dahari, M., Kazi, S.N., "*Study of synthesis, stability and thermophysical properties of graphene nanoplatelet/platinum hybrid nanofluid*", International Communications in Heat and Mass Transfer, Vol. 77, pp. 15-21, 2016, doi: 10.1016/j.icheatmasstransfer.2016.07.010.

[29]Bahiraei, M., Heshmatian, S., "*Efficacy of a novel liquid block working with a nanofluid containing graphene nanoplatelets decorated with silver nanoparticles compared with conventional CPU coolers*", Applied Thermal Engineering, Vol. 127, pp. 1233-1245, 2017, doi: 10.1016/j.applthermaleng.2017.08.136.

[30]Yarmand, H., Zulkifli, N.W.B.M, Gharehkhani, S., Shirazi, S.F.S., Alrashed, A.A.A.A., Ali, M.A.B., Dahari, M., Kazi, S.N., "*Convective heat transfer enhancement with graphene nanoplatelet/platinum hybrid nanofluid*", International Communications in Heat and Mass Transfer, Vol. 88, pp. 120-125,2017, doi: 10.1016/j.icheatmasstransfer.2017.08.010.

[31]Bahiraei, M., Heshmatian, S., "*Thermal performance and second law characteristics of two new microchannel heat sinks operated with hybrid nanofluid containing graphene–silver nanoparticles*", Energy Conversion and Management, Vol. 168, pp. 357-370, 2018, doi: 10.1016/j.enconman.2018.05.020.

[32]Bahiraei, M., Mazaheri, N.,"*Application of a novel hybrid nanofluid containing graphene–platinum nanoparticles in a chaotic twisted geometry for utilization in miniature devices: thermal and energy efficiency considerations*". International Journal of Mechanical Sciences, Vol. 138-139. pp. 337–349, 2018, doi: 10.1016/j.ijmecsci.2018.02.030.

[33]Bahiraei, M., Jamshidmofid, M., Goodarzi, M., "*Efficacy of a hybrid nanofluid in a new microchannel heat sink equipped with both secondary channels and ribs*", Journal of Molecular Liquids, Vol. 273, pp. 88-98, 2019, doi: 10.1016/j.molliq.2018.10.003.

[34]Khosravi, R., Rabiei, S., Bahiraei, M., Teymourtash, A.R., "*Predicting entropy generation of a hybrid nanofluid containing graphene–platinum nanoparticles through a microchannel liquid block using neural networks*",

International Communications in Heat and Mass Transfer, Vol. 109, pp. 104351, 2019, doi: 10.1016/j.icheatmasstransfer.2019.104351.

[35] Bahiraei, M., Mazaheri, N., Hassanzamani, S.M.S., "*Efficacy of a new graphene–platinum nanofluid in tubes fitted with single and twin twisted tapes regarding counter and co-swirling flows for efficient use of energy*", International Journal of Mechanical Sciences, Vol. 150, pp. 290-303, 2019, doi: 10.1016/j.ijmecsci.2018.10.036.

[36] Bahiraei, M., Mazaheri, N., Rizehvandi, A., "*Application of a hybrid nanofluid containing graphene nanoplatelet–platinum composite powder in a triple-tube heat exchanger equipped with inserted ribs*", Applied Thermal Engineering, Vol. 149, pp. 588-601, 2019, doi: 10.1016/j.applthermaleng.2018.12.072.

[37] Goodarzi, M., Tlili, I., Tian, Z., Safaei, M.R., "*Efficiency assessment of using graphene nanoplatelets-silver/water nanofluids in microchannel heat sinks with different cross-sections for electronics cooling*", International Journal of Numerical Methods for Heat & Fluid Flow, Vol. 30, pp. 347-372, 2020, doi: 10.1108/HFF-12-2018-0730.

[38] Balaji, T., Selvam, C., Mohan Lal, D., Harish, S., "*Enhanced heat transport behavior of microchannel heat sink with graphene based nanofluids*", International Communications in Heat and Mass Transfer, Vol. 117, pp. 104716, 2020, doi: 10.1016/j.icheatmasstransfer.2020.104716.

[39] Khosravi, R., Teymourtash, A.R., Passandideh Fard, M., Rabiei, S., Bahiraei, M., "*Numerical study and optimization of thermohydraulic characteristics of a graphene–platinum nanofluid in finned annulus using genetic algorithm combined with decision-making technique*", Engineering with Computers, Vol. 37, pp. 2473–2491, 2021, doi: 10.1007/s00366-020-01178-6.

[40] Glassbrenner, C.J., Slack, G.A., "*Thermal Conductivity of Silicon and Germanium from 3K to the Melting Point*", Physical Review. Vol. 134, pp. 1058-1069, 1964. doi: 10.1103/PhysRev.134.A1058.